



## Selective oxidation of ethanol into acetaldehyde catalyzed by a novel Mg-Mo/MCM-41 mesoporous molecular sieves

P. M. Cocha-Vesga<sup>a,b\*</sup> • N. Rojas-Arias<sup>a,c\*\*</sup> • G. P. Valença<sup>b</sup>

<sup>a</sup>Universidad Pedagógica y Tecnológica de Colombia,  
Departamento de Ingeniería Metalúrgica, 150003, Tunja-Boyacá, Colombia

<sup>b</sup>Universidade Estadual de Campinas,  
Laboratório para Estudos de Processos de Adsorção e Catálise, Campinas-SP, Brasil

<sup>c</sup>Postgraduate Program in Materials Science and Engineering,  
Federal University of São Carlos 1356-905, São Carlos, Brazil

Received 02 25 2021; accepted 10 04 2021

Available 02 28 2022

**Abstract:** MCM-41 mesoporous molecular sieves impregnated with MgO, MoO<sub>3</sub>, and Mo<sub>2</sub>C were synthesized using a wet impregnation method. The compounds developed herein, were characterized by means of XRD, SEM-EDS and FT-IR techniques. The production capacity of acetaldehyde from ethanol was analyzed by catalytic processes employing as-synthesized MCM-41. The obtained results show that the changes in crystallinity of MCM-41 were generated by the impregnation of oxides, which generate damage to the structure of MCM-41. Nevertheless, the characteristics of the compounds show a favorable reactivity behavior, allowing them to be used as heterogeneous catalyst material due to the similarity of the characteristics between MCM-41 with and without Mg and Mo oxides. The catalytic tests show the influence between the type of catalyst used and the temperature applied to the selective process of acetaldehyde from ethanol, obtaining the best results in the samples impregnated with Mo<sub>2</sub>C at 250 °C, with a production percentage of acetaldehyde of 80.7% and 77.9% for the catalysts impregnated with 0.5% and 2.0% Mg and 3.0% Mo carbide, respectively.

**Keywords:** MCM-41 mesoporous molecular sieve, ethanol, catalytic process, acetaldehyde

\*Corresponding author.

E-mail address: pablo.coha@uptc.edu.co, nicolas.rojas@estudante.ufscar.br (P.M. Cocha-Vesga, N. Rojas-Arias).

Peer Review under the responsibility of Universidad Nacional Autónoma de México.

## 1. Introduction

Ethanol has become a promising candidate to replace fossil fuels (Sun & Wang, 2014). The production of ethanol also allows its implementation in the generation of chemicals such as acetaldehyde (Cánepa et al., 2020; Klinthongchai et al., 2020), which is used in a wide variety of industrial applications (Rosales-Calderon & Arantes, 2019). Several processes of converting ethanol to acetaldehyde usually requires oxidation processes in the liquid phase, using homogeneous catalysts (Jira, 2009); however, the catalysts applied to suffer a high deactivation rate, for which the process has not been very successful. This has aroused interest in the application of different heterogeneous catalysts that allow increasing the yield during the process of converting ethanol to acetaldehyde. The application of MCM-41 porous material systems have showed optimal results during the selective oxidation process (Cánepa et al., 2020).

The MCM-41 meso-porous material is a type of porous material with pore sizes between 2 nm and 50 nm that has been widely accepted due to its unique properties and potential applications, maintaining the same advantages of a conventional porous material (Beck et al., 1992; Kishor & Ghoshal, 2017; Kresge et al., 1992; Ramazani et al., 2019; Wang et al., 2012). Several authors have used different mechanisms for the manufacture of porous materials MCM-41, applying new raw materials such as organic materials and certain minerals, e.g. bentonite (Liang et al., 2017; Liu et al., 2020; Liu et al., 2019; Yang et al., 2018). Nevertheless, the management of manufacturing techniques with traditional reagents is still in force.

The application of this type of materials in catalytic activities has a great impact. The application of metals such as Cu, Mn, and Mg supported in MCM-41 have a great reaction activity compared to other catalysts (Li et al., 2006; Li et al., 2008; Mukherjee et al., 2019). The replacement of homogeneous catalysts with heterogeneous catalysts has attracted much attention due to the easy separation of catalyst products, as well as the possible regeneration and reuse of heterogeneous catalysts (Wang et al., 2012). The physical properties of MCM-41 related to its structure diversity and porosity allow this material to be a suitable choice as a carrier (Zhang et al., 2010; Zheng et al., 2020).

Recently, transition metal catalysts, such as Cu, Mn, Mo, Fe, Cr, Co, and their oxides are widely studied (Lopez et al., 2016; Li et al., 2006). However, several of these metals are considered highly toxic, which makes them impractical for wide adoption in various catalytic processes. Among them Mg have been recognized as a new non-toxic material that allows the adsorption and removal of metal ions and organic pollutants

from dirty waters due to the fact that  $O^{2-}$  radicals favor the degradation of these components (Sharma & Kakkar, 2017). The combination of MgO or Mo with MCM-41 improves the properties of each compound, allowing a greater scope of application (Gui et al., 2015; Higashimoto et al., 2005; Mohamed et al., 2017; Peng et al., 2016; Safa & Ma, 2016; Saraiva et al., 2014; Stefanidis et al., 2016). Nevertheless, few studies have been reported with Mg and Mo for the formation of inter-metallic compounds supported in MCM-41 (Barthos et al., 2008; Costa et al., 2020).

Ethanol is a derivative of biomass that has been widely accepted as a material to replace conventional fossil fuels (Sun & Wang, 2014), and different products of interest such as acetaldehyde can be produced through it (Rodriguez-Gomez et al., 2017; Shan et al., 2017; Shan et al., 2018). For this reason, the purpose of this work is to develop the synthesis and characterization of MCM-41 mesoporous sieves impregnated with Mg and Mo oxides that will serve as catalysts in the production of acetaldehyde from ethanol, since this compound can be widely used in different applications e.g., perfumery, flavorings, aniline dyes, plastics, hardening of gelatinous fibers, fertilizers, chemical compounds, and so on (Luttrell, 2009). The procedure of this study consists the manufacture and impregnation of Mg oxides and Mo oxides and their carbides within the structure of the MCM-41 material. This procedure allowed to determine the influence of Mo and Mg within the physical characteristics of MCM-41.

## 2. Experimental

### 2.1. Catalyst preparation

A series of six catalyst materials were synthesized in this study. The catalysts were synthesized with magnesium oxide at 0.5wt%, 1.0wt% and 2.0wt% produced from precursor salts by means of the wet impregnation method. The magnesium oxide (MgO) catalysts were doped with 3wt% molybdenum in the form of oxide ( $MoO_3$ ) and carbide ( $Mo_2C$ ). The six catalyst are presented in the Table 1.

Table 1. Catalyst produced in this work.

Additives	Composition [wt%]
Mo Oxide	MCM-41 0.5% Mg 3.0% Mo
	MCM-41 1.0% Mg 3.0% Mo
	MCM-41 2.0% Mg 3.0% Mo
Mo Carbide	C-MCM-41 0.5% Mg 3.0% Mo
	C-MCM-41 1.0% Mg 3.0% Mo
	C-MCM-41 2.0% Mg 3.0% Mo

## 2.2. MCM-41 molecular sieve

The MCM-41 mesoporous sieves were synthesized by using tetraethyl orthosilicate ( $\text{SiC}_8\text{H}_{20}\text{O}_4$ ) (Sigma Aldrich, 99.0% purity) as a silica source and cetyltrimethylammonium bromide ( $\text{C}_{16}\text{H}_{33}(\text{CH}_3)_3\text{NBr}$ ) (Sigma Aldrich, 99.0% purity) as template (Pires et al., 2002; Uphade et al., 2001). A 630 mL amount of ammonium hydroxide ( $\text{NH}_4\text{OH}$ ) (Merck, 25% analytical purity) was used with 810 mL of deionized water. Subsequently, 6 g of  $\text{C}_{16}\text{H}_{33}(\text{CH}_3)_3\text{NBr}$  and 30 mL of  $\text{SiC}_8\text{H}_{20}\text{O}_4$  were added. The mixture was stirred on a mechanical shaker at 420 rpm during 2 h at room temperature, maintaining the pH = 12 in the solution. Subsequently, the solution was vacuum filtered and dried in an electric oven at 127 °C for 24 h. The dried samples were calcined at 600 °C for 11 h in a ½" internal diameter U-shaped quartz tube furnace. The first 5 h of the calcination process were carried out under a nitrogen flow of 100 mL·min<sup>-1</sup> while the rest of the process (6 h) was carried out under an air flow of 100 mL·min<sup>-1</sup> (Paloschi, 2002).

## 2.3. Mg impregnation

The addition of Mg to the developed samples was carried out by the wet impregnation method, using a solution of magnesium nitrate ( $\text{Mg}(\text{NO}_3)_2 \cdot 6\text{H}_2\text{O}$ ) (99.0% purity). The MCM-41 samples were used as a substrate in this process. The solutions were manufactured by varying the nitrate percentage to obtain 0.5, 1.0, and 2.0 (in wt.%) of Mg in the solution. The mixtures were stirred at 420 rpm for 2 h to ensure the homogeneous dissolution of the reagents in the solution. The solution was dried in an electric oven at 127 °C for 12 h; subsequently, the solid material was calcined at 600°C for 5 h with air flow (Vinu et al., 2004; Yasyerli et al., 2011).

## 2.4. Mo impregnation

The molybdenum addition was made from molybdenum oxides in half of the samples and in the form of molybdenum carbide for the remaining samples. The percentage used was 3wt% in both samples. Molybdenum oxide was prepared by adding a solution of ammonium heptamolybdate ( $(\text{NH}_4)_6\text{Mo}_7\text{O}_{24}$ ) (99.0% purity) by the wet impregnation method. A mixture of 1.0 g of MCM-41 impregnated with Mg, 0.4 g of  $(\text{NH}_4)_6\text{Mo}_7\text{O}_{24}$ , and 10 mL of deionized water was prepared. The sample obtained was vacuum filtered and dried at 127 °C for 12 h. Thereafter, the samples were calcined at 500 °C for 7 h with air flow (Higashimoto et al., 2005; Medeiros & Appel, 2002; Rana & Viswanathan, 1998).

For the preparation of the samples with molybdenum carbide, the  $(\text{NH}_4)_6\text{Mo}_7\text{O}_{24}$  was treated with a mixture of natural gas and hydrogen (80 %  $\text{CH}_4$  – 20 %  $\text{H}_2$ ). The samples were calcined at 627 °C for 3 h. After complete preparation of carbide, the catalysts were cleaned of surface polymeric carbon with a flow of  $\text{H}_2$  at 727 °C (unclear sentence). Manufacture of the carbide was done on-site because the catalyst is very sensitive towards air and can be decomposed

in contact with air (Cai et al., 2011; Farkas & Solymosi, 2007; Santos, 2002; Zhao et al., 2010).

## 2.5. Catalyst characterization

The characterizations of the sintered samples were carried out by means of powder X-ray diffraction techniques, using a source of Cu K $\alpha$  ( $\lambda = 0.15406$  nm), 40 kV and 30 mA, a  $2\theta$  scale from 1.5 ° to 70 ° and a step of 0.04 °·s<sup>-1</sup>; Fourier transform infrared (FT-IR) spectroscopy on a Thermo Scientific equipment, model Nicolet-6700, between the range of 4000 to 400 cm<sup>-1</sup> with a step of 4 cm<sup>-1</sup>; and scanning electron microscopy (SEM) using a ZEISS LEO 440 Scanning Electron Microscope (SEM) and corresponding Energy Dispersed X-ray Spectroscopy (EDS) technique at 10k magnification.

## 2.6. Catalyst behavior

Prior to the catalysis tests, the catalyst materials were cleaned at 300 °C using a flow of nitrogen gas at 60 mL·min<sup>-1</sup> for one hour following a mixture of nitrogen at 60 mL·min<sup>-1</sup> and oxygen at 20 mL·min<sup>-1</sup> and finally by a nitrogen flow at 120 mL·min<sup>-1</sup>. This process was carried out to guarantee the removal of particles and possible contaminants from the samples.

The catalytic activity of ethanol used for the acetaldehyde formation was tested using a gas phase reaction. The process was carried out in a stream of nitrogen saturated – ethanol with a flow of 60 mL·min<sup>-1</sup>. A constant amount (0.03 g) of each catalyst was used, while varying the temperature from 200 °C to 300 °C in interval of 25 °C. The tests were carried out for a period of 4 h for each of the samples, maintaining a constant pressure of 7.870 kPa for the ethanol. Three replications were made for each of the samples for a total of 90 tests.

## 3. Results and discussion

The samples prepared and sintered to obtain MCM-41 compounds impregnated with MgO and Mo, in the form of oxide ( $\text{MoO}_3$ ) and carbide ( $\text{Mo}_2\text{C}$ ), were developed by hydrothermal synthesis method. In that way, the composite materials obtained were analyzed using different techniques. The obtained data is represented in the form of graphs for each of the characterization techniques used in order to show the behavior in the sintered materials.

### 3.1. X-ray diffraction (XRD)

The XRD patterns are presented in Figure 1. The graphs show the diffraction spectra for the samples of pure MCM-41 (Figure 1(a)), where the main peaks of the MCM-41 structure can be seen. In Figure 1(b) the samples of MCM-41 impregnated with  $\text{MoO}_3$  and in Figure 1(c) the samples of MCM-41 impregnated with  $\text{Mo}_2\text{C}$ . The diffraction peaks for the pure MCM-41 molecular sieve sample (Figure 1(a)) are clearly observed at 100 ( $2\theta = 1.9^\circ$ ); 110 ( $2\theta = 3.6^\circ$ ) and 200 ( $2\theta = 4.2^\circ$ ) which show

a behavior according to other patterns published by other authors for this material (Bentahar et al., 2017; Liu et al., 2020). These peaks will serve as a reference standard for the analysis of MCM-41 samples impregnated with MgO and Mo in oxide and carbide form.

Figure 1(b) shows the diffraction patterns obtained for the MCM-41 samples impregnated with Mg and Mo oxides. MoO<sub>3</sub> could be observed in the XRD patterns, showing that the impregnation and calcination methods were successful. The MgO pattern cannot be clearly seen due to the low percentage of it in the samples. The impregnation of the samples later with MoO<sub>3</sub> was able to hide the dispersed magnesium that is incorporated into the MCM-41, preventing a signal from it from being generated during the XRD analysis (Fang et al., 2020; Liu et al., 2010). Figure 1(c) shows the diffraction patterns for the Mo<sub>2</sub>C-impregnated samples. The peaks corresponding to MgO were not also exhibited in this graph. However, the Mo<sub>2</sub>C peaks are visible in each of the analyzed samples, indicating that this process was also carried out successfully. The low percentages of Mo<sub>2</sub>C favored the impregnation process on the MCM-41 molecular sieve.

Figure 1(b – c) show a partially crystalline material, with the presence of amorphous material, mainly between the 15 ° to 35 ° angles of the diffraction patterns, found in each of the analyzed samples. This amorphous content can be attributed to the MCM-41 molecular sieve which presents, in its pure state and free of impregnation (Figure 1(a)), a partially amorphous zone in its spectrum in a range of angle window similar to those found in Figure 1(b) and Figure 1(c). Nevertheless, the impregnation of oxidized compounds, such as the contribution of Mo from oxides, can favor an increase in the amorphous content of the material. The calcination of compounds could generate losses of some compounds due to volatilization processes, affecting part of the structure of MCM-41. The presence of a low percentage of Mg within the material favors the catalytic properties of the material without affecting other physical properties such as its structure or pH (Barthos et al., 2008).

The variation and increase of Mo in the samples, whether in the form of oxide or carbide, does not greatly affect the crystalline structure of the sintered materials. Although all the samples partially conserved the general structure of MCM-41 as also presented by other authors (Sikarwar et al., 2018), the handling of an oxide or carbide for the contribution of Mo during the synthesis process allows to vary the type of structure and crystallinity of the material.

### 3.2. B. FT-IR characterization

FT-IR analysis was performed on the synthesized catalysts. The results are presented in Figure 2. By means of this technique it is possible to determine by wavelength the link

between the elements present in each one of the synthesized samples. The graphs show bands at 450 cm<sup>-1</sup> and 1092 cm<sup>-1</sup> in Figure 2(a – b). These correspond to a Si – O – Si bond, typical of the MCM-41 sieve. The bands at 560 cm<sup>-1</sup> can be analyzed as preliminary criteria to affirm the formation of a solid ordered structure (Pirouzmand, Anakhatoon, et al., 2018; Pirouzmand, Asadi, et al., 2018). Additionally, in Figure 2(a) bands can be observed at 960 cm<sup>-1</sup> corresponding to the vibrations of a Metal – O – Si bond and peaks at 905 cm<sup>-1</sup>, which correspond to the vibrations of the Mo – O bond. These last two bands indicate the strong presence of molybdenum oxide and magnesium oxide in the analyzed samples. Nevertheless, in Figure 2(b) all bands corresponding to molybdenum oxide disappear, showing that the molybdenum species had been converted to molybdenum carbide.

### 3.3. SEM-EDS characterization

The images obtained by SEM allow to observe that all samples presented a similar morphology, characteristic to the MCM-41 sieves. Figure 3 shows an example of the morphology found in the synthesized samples. The formation of spherical compact particles with a regular format can be observed, similar to other Mg/MCM-41 compounds, which show a greater degree of agglomeration by the particles (Karnjanakom et al., 2017). The union of these particles presents a partial melting behavior (free of agglomerations) due to the synthesis and calcination processes, which were carried out at moderately high temperatures, allowing the melting and partial union of these particles (Figure 3). It was verified that there were no agglomerations of particles, which would be a consequence of calcination (Borrell, 2010). This morphology is in good agreement with previously reported data (Sikarwar et al., 2018).

The elemental composition analyzes were carried out using the Energy Disperse X-ray Spectroscopy (EDS) technique. The results obtained by this technique are shown in Figure 4. The data obtained show all the expected elements, finding the presence of Si and O, characteristics of MCM-41, as well as Mg, Mo, and C, typical of the materials used during the impregnation process. Figure 4(a – c) are the samples worked with MgO and MoO<sub>3</sub> as starting materials EDS measurements allow observing the presence of Mg and Mo elements. Similarly, Figure 4(d – f) correspond to catalysts with MgO and Mo<sub>2</sub>C carbide, which not only show the presence of Mg and Mo, but also show the presence of C, and it corresponds to the molybdenum carbide used during the synthesis process. The generation of a heterogeneous catalyst, favors certain properties such as the capacity for regeneration and reuse, sought today for new materials (Jin et al., 2012; Vinu et al., 2004; Wang et al., 2012).

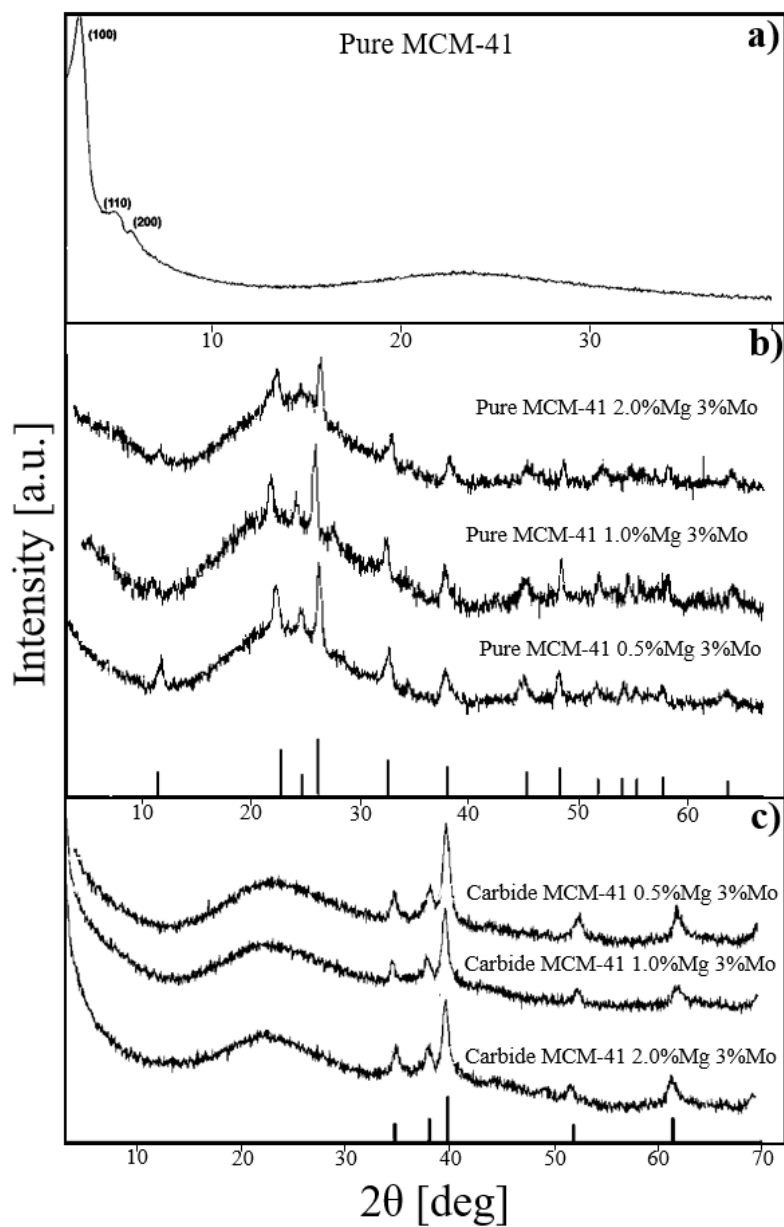


Figure 1. XRD patterns for synthesized catalysts obtained in this work. In a) for pure MCM-41 molecular sieve, b) MCM-41 molecular sieve impregnated with Mg and Mo oxides, and c) MCM-41 molecular sieve impregnated with Mg oxide and Mo carbide.

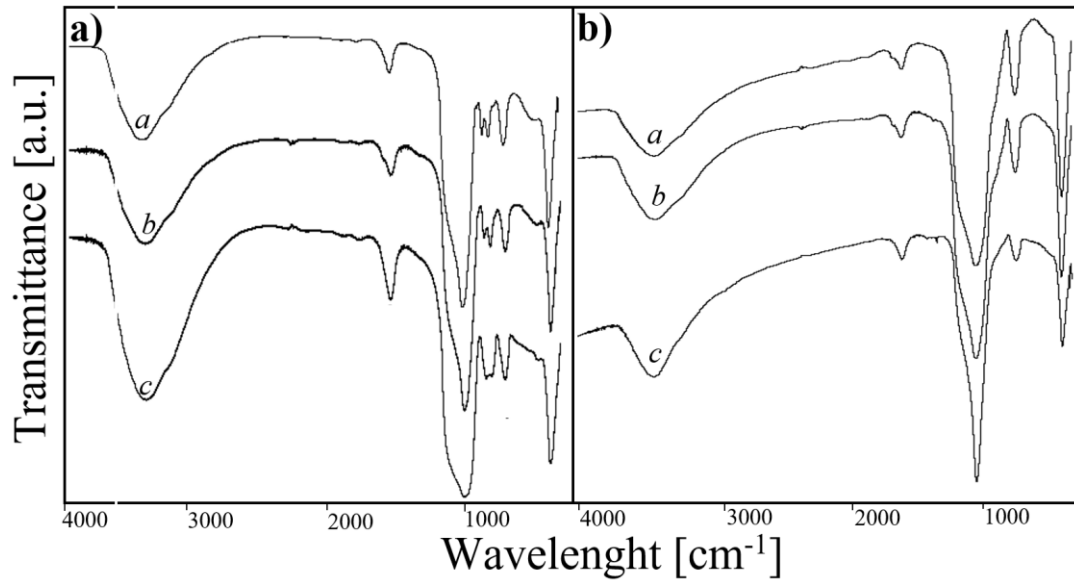


Figure 2. FT-IR analysis realized for a) MCM-41 impregnated with Mg and Mo oxides, and b) MCM-41 impregnated with Mg oxide and Mo carbide.

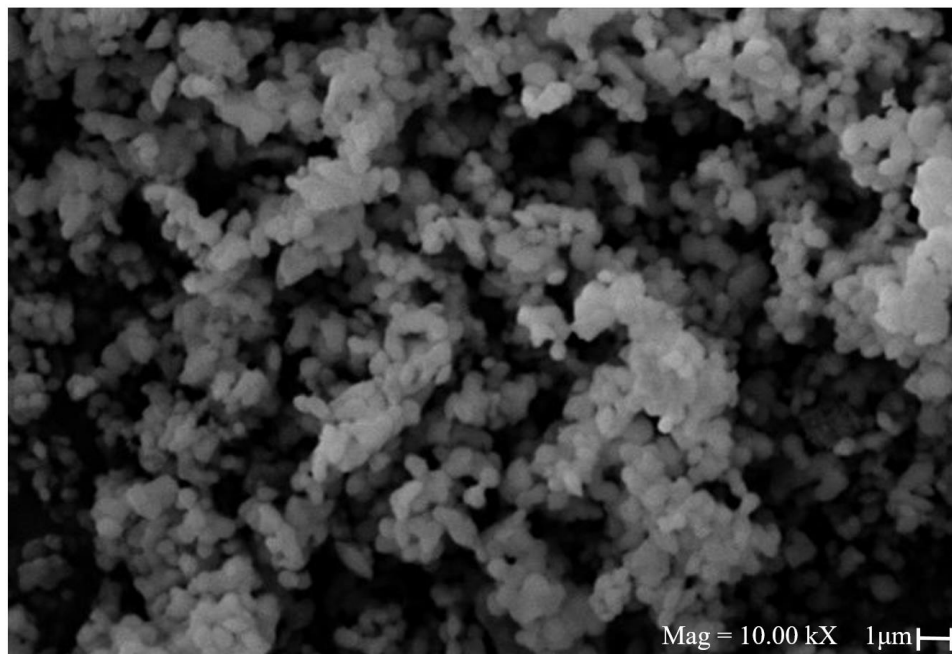


Figure 3. SEM image obtained for a pure MCM-41 impregnated with Mg oxide and Mo carbide.

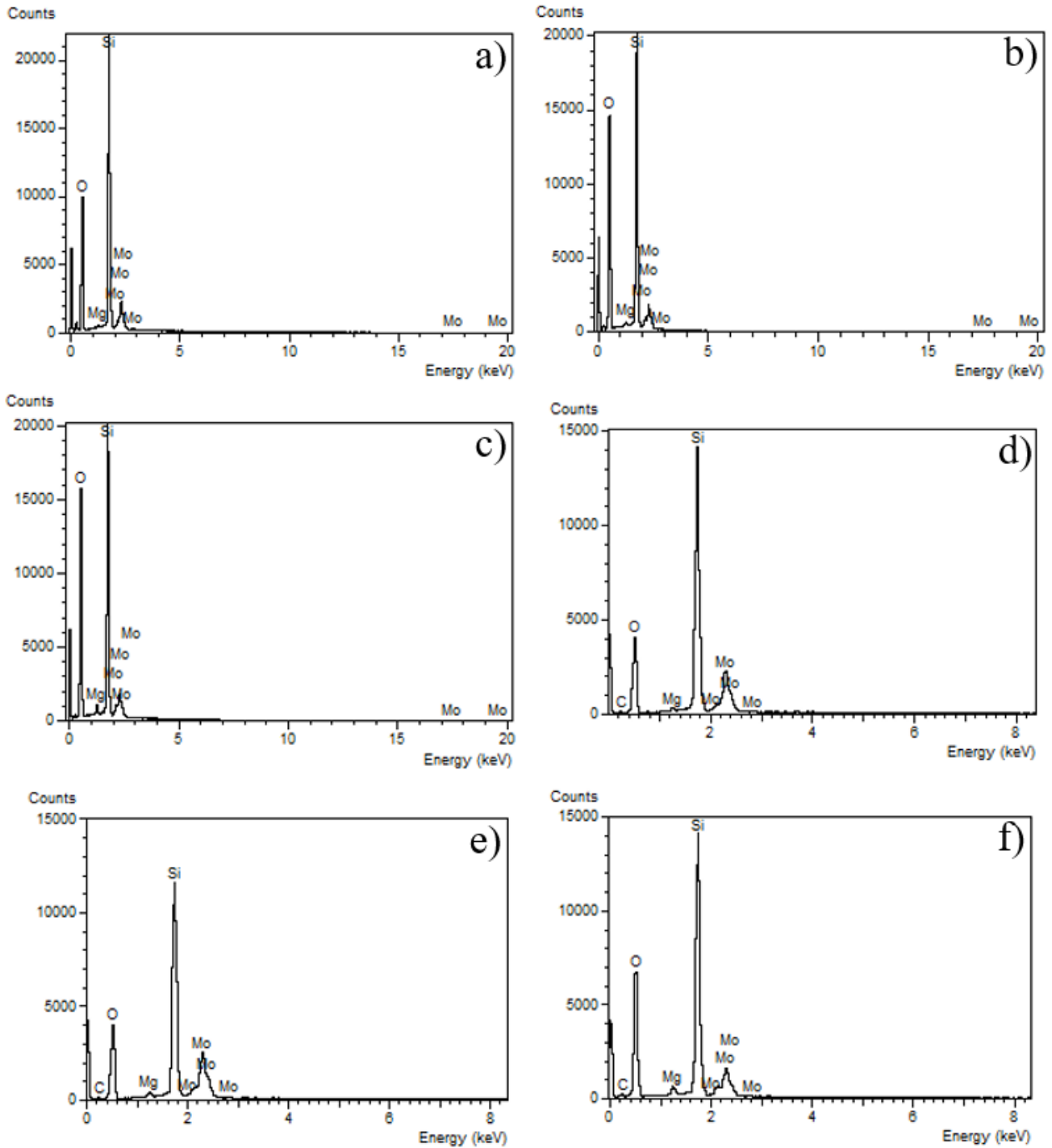


Figure 4. EDS analysis realized for the samples produced in this work. In a), b), and c) are the samples worked with Mg and Mo oxide. In e), f) and g) the samples worked with Mg oxide and Mo carbide.

### 3.4. Tests with the catalysts.

The data obtained in this stage allowed to observe the degree of ethanol conversion, as well as the percentage of acetaldehyde production using the different types of catalysts. The conversion profile of the catalysts used is presented in Figure 5. The increase in temperature favors the conversion of ethanol into other products, with the highest performance observed in catalysts impregnated with molybdenum carbide. At the temperature of 300 °C, a maximum conversion value of 31% is achieved in the MCM-41 catalyst impregnated with 0.5% Mg-3.0% Mo. An increase in Mg within the MCM-41 catalyst generates a reduction during the process of conversion of ethanol with an average conversion value of 25.52% in the catalyst impregnated with 2.0% Mg. The application of Molybdenum in oxide form can generate a reduction in the degree of conversion of up to 21%.

Using Pearson's correlation methods, it is observed that the catalyst sample produced with 0.5% Mg-3.0% Mo has a greater relationship between the increase in temperature and the degree of conversion of ethanol gas into other products, the catalysts produced with the addition of Mo in the form of carbide present a direct correlation with the temperature of 95.1% on average, obtaining a value of 96.2% in the catalyst with 0.5% Mg-3.0% Mo. On the other hand, the catalysts produced with MoO<sub>3</sub> show only a direct ratio of 87.2%. Temperature has an influence on the reaction and conversion of ethanol, the composition of the samples being more

important. In this sense, the application of molecular sieves impregnated with molybdenum in the form of carbide and in low percentages, i.e. MCM-41 carbide 0.5% Mg-3.0% Mo, favors the conversion process of ethanol, while the compound such as MCM-41 2.0% Mg-3.0% Mo showed inferior activity.

Figure 6 shows the percentage of acetaldehyde generated during the catalytic tests using the different catalysts produced. Variations between samples are observed on acetaldehyde synthesis from ethanol during the catalysis process. The catalysts impregnated with cobalt carbide showed the best performance, mainly at 250 °C. The MCM-41 1.0% Mg-3.0% Mo catalyst samples presented their best performance at a temperature at 200°C, obtaining a production of acetaldehyde up to 79.8%. An increase the temperature causes a reduction in acetaldehyde production up to 10%. On the other hand, the catalysts impregnated with 0.5% and 2.0% MgO and 3.0% Mo<sub>2</sub>C presented their highest production values at 250 °C, with a production percentage of acetaldehyde of 80.7% and 77.9%, respectively. The correlation of the obtained data shows that temperature has a greater influence on the MCM-41 catalyst sample, 0.5% Mg and 3.0% Mo in oxide form, with a correlation up to 97.7%. The catalysts with 2.0% Mg-3.0% Mo in the oxide form and 1.0% Mg-3.0% Mo oxide obtained a correlation of 79.5%, indicating a positive correlation for the sample impregnated with Mo oxide and negative for Mo carbide. The other catalysts produced in this study show a degree of correlation of less than 40%.

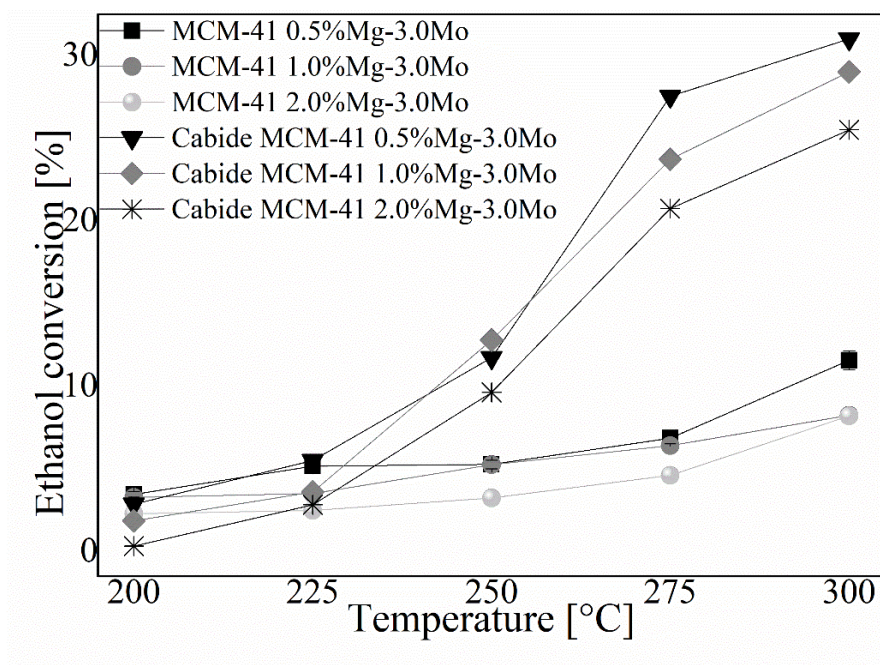


Figure 5. SEM image obtained for a pure MCM-41 impregnated with Mg oxide and Mo carbide.

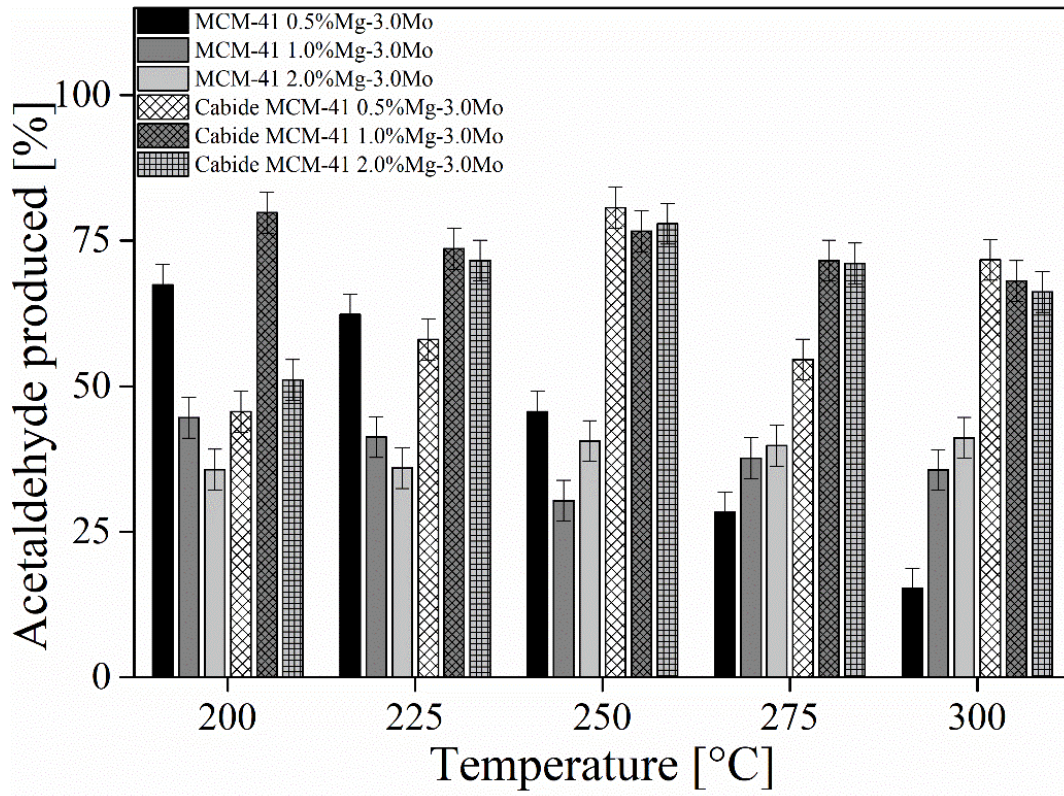


Figure 6. Percentage of acetaldehyde generated during the catalysis tests using the different catalysts produced.

#### 4. Conclusions

The pristine MCM-41 and MCM-41 impregnated with Mg and Mo were synthesized using the methodology described in the document. The techniques used for characterization allowed observing the status and relationship of each of the samples developed in this study. The data obtained by the FT-IR techniques allowed us to observe that the MCM-41 samples impregnated with Mg and Mo largely conserve the characteristics of the MCM-41 molecular sieve, while the XRD standards and the SEM-EDS images showed a change in the crystallinity and structure of the samples when developed with oxides or carbides of Mo. The SEM images allowed observing the mechanism of union of the components used. In addition, the presence of spherical particles maintains a

union due to a partial fusion generated during the synthesis process and the temperature at which it was carried out, allowing the partial union of the particles without reaching a total fusion state or agglomeration.

Catalytic tests show an improvement in the degree of selective and production of acetaldehyde from ethanol when the MCM-41 are impregnated with Mo carbide. The ethanol conversion during the catalysis process was highly related to the increase in temperature, obtaining a degree of correlation up to 95.1% in the samples impregnated with Mo carbide and 87.2% in the samples impregnated with Mo oxide. However, the highest degree of acetaldehyde production was found at 250 °C for the MCM-41 1.0% Mg catalyst impregnated with 3.0% Mo carbide.

## Conflict of interest

The author(s) does/do not have any type of conflict of interest to declare.

## Acknowledgments

The support given by CAPES (the University of Campinas) and the Universidad Pedagógica y Tecnológica de Colombia, by providing material and equipment necessary for the research, is greatly appreciated.

## Financing

The authors did not receive any sponsorship to carry out the research reported in the present manuscript

## References

- Barthos, R., Széchenyi, A., & Solymosi, F. (2008). Efficient H<sub>2</sub> Production from Ethanol over Mo<sub>2</sub>C/C Nanotube Catalyst. *Catalysis Letters*, 120(3–4), 161–165. <https://doi.org/10.1007/s10562-007-9265-8>
- Beck, J. S., Vartuli, J. C., Roth, W. J., Leonowicz, M. E., Kresge, C. T., Schmitt, K. D., & Schlenker, J. (1992). A new family of mesoporous molecular sieves prepared with liquid crystal templates. *Journal of the American Chemical Society*, 114(27), 10834–10843. <https://doi.org/10.1021/ja00053a020>
- Bentahar, S., Dbik, A., Khomri, M. El, Messaoudi, N. El, & Lacherai, A. (2017). Adsorption of methylene blue, crystal violet and congo red from binary and ternary systems with natural clay: Kinetic, isotherm, and thermodynamic. *Journal of Environmental Chemical Engineering*, 5(6), 5921–5932. <https://doi.org/10.1016/j.jece.2017.11.003>
- Borrell T. A. (2010). *Nuevos materiales ultrafuncionales: Cerámica/nanofibras de carbono*. [tesis, Universidad de Oviedo]. Repositorio UO. <http://hdl.handle.net/10651/12840>
- Cai, C., Wang, H., & Han, J. (2011). Synthesis and characterization of ionic liquid-functionalized aluminosilicate MCM-41 hybrid mesoporous materials. *Applied Surface Science*, 257(23), 9802–9808. <https://doi.org/10.1016/j.apsusc.2011.06.025>
- Cánepa, A. L., Vaschetti, V. M., Pájaro, K. C., Eimer, G. A., Casuscelli, S. G., & Cortés Corberán, V. (2020). Selective oxidation of ethanol on V-MCM-41 catalysts. *Catalysis Today*, 356, 464–470. <https://doi.org/10.1016/j.cattod.2019.09.052>
- Costa, J. A. S., de Jesus, R. A., Santos, D. O., Mano, J. F., Romão, L. P. C., & Paranhos, C. M. (2020). Recent progresses in the adsorption of organic, inorganic, and gas compounds by MCM-41-based mesoporous materials. *Microporous and Mesoporous Materials*, 291, 109698. <https://doi.org/10.1016/j.micromeso.2019.109698>
- Fang, Y., Li, J., Sheng, N., Wang, X., Chen, D., Cai, M., ... & Dai, L. (2020). Enhanced catalytic oxidation of anthracene by deposition of MoO<sub>3</sub> and WO<sub>3</sub> nanoparticles on MCM-41. *Molecular Catalysis*, 497, 111209. <https://doi.org/10.1016/j.mcat.2020.111209>
- Farkas, A. P., & Solymosi, F. (2007). Adsorption and reactions of ethanol on Mo<sub>2</sub>C/Mo(100). *Surface Science*, 601(1), 193–200. <https://doi.org/10.1016/j.susc.2006.09.023>
- Gui, C. X., Li, Q. J., Lv, L. L., Qu, J., Wang, Q. Q., Hao, S. M., & Yu, Z. Z. (2015). Core-shell structured MgO@ mesoporous silica spheres for enhanced adsorption of methylene blue and lead ions. *RSC Advances*, 5(26), 20440–20445. <https://doi.org/10.1039/C5RA02596F>
- Higashimoto, S., Hu, Y., Tsumura, R., Iino, K., Matsuoka, M., Yamashita, H., ... & Anpo, M. (2005). Synthesis, characterization and photocatalytic reactivities of Mo-MCM-41 mesoporous molecular sieves: Effect of the Mo content on the local structures of Mo-oxides. *Journal of Catalysis*, 235(2), 272–278.
- Jin, S., Cui, K., Guan, H., Yang, M., Liu, L., & Lan, C. (2012). Preparation of mesoporous MCM-41 from natural sepiolite and its catalytic activity of cracking waste polystyrene plastics. *Applied Clay Science*, 56, 1–6. <https://doi.org/10.1016/j.clay.2011.11.012>
- Jira, R. (2009). Acetaldehyde from Ethylene-A Retrospective on the Discovery of the Wacker Process. *Angewandte Chemie International Edition*, 48(48), 9034–9037. <https://doi.org/10.1002/anie.200903992>
- Karnjanakom, S., Suriya-umporn, T., Bayu, A., Kongparakul, S., Samart, C., Fushimi, C., Abudula, A., & Guan, G. (2017). High selectivity and stability of Mg-doped Al-MCM-41 for in-situ catalytic upgrading fast pyrolysis bio-oil. *Energy Conversion and Management*, 142, 272–285. <https://doi.org/10.1016/j.enconman.2017.03.049>
- Kishor, R., & Ghoshal, A. K. (2017). Amine-Modified Mesoporous Silica for CO<sub>2</sub> Adsorption: The Role of Structural Parameters. *Industrial & Engineering Chemistry Research*, 56(20), 6078–6087. <https://doi.org/10.1021/acs.iecr.7b00890>

- Klinthongchai, Y., Prichanont, S., Praserttham, P., & Jongsomjit, B. (2020). Synthesis, characteristics and application of mesocellular foam carbon (MCF-C) as catalyst for dehydrogenation of ethanol to acetaldehyde. *Journal of Environmental Chemical Engineering*, 8(3), 103752. <https://doi.org/10.1016/j.jece.2020.103752>
- Kresge, C. T., Leonowicz, M. E., Roth, W. J., Vartuli, J. C., & Beck, J. S. (1992). Ordered mesoporous molecular sieves synthesized by a liquid-crystal template mechanism. *Nature*, 359(6397), 710–712. <https://doi.org/10.1038/359710a0>
- Li, W. B., Zhuang, M., & Wang, J. X. (2008). Catalytic combustion of toluene on Cu-Mn/MCM-41 catalysts: Influence of calcination temperature and operating conditions on the catalytic activity. *Catalysis Today*, 137(2–4), 340–344. <https://doi.org/10.1016/j.cattod.2007.11.002>
- Li, W. B., Zhuang, M., Xiao, T. C., & Green, M. L. H. (2006). MCM-41 Supported Cu-Mn Catalysts for Catalytic Oxidation of Toluene at Low Temperatures. *The Journal of Physical Chemistry B*, 110(43), 21568–21571. <https://doi.org/10.1021/jp063580g>
- Liang, Z., Zhao, Z., Sun, T., Shi, W., & Cui, F. (2017). Enhanced adsorption of the cationic dyes in the spherical CuO/mesoporous silica nano composite and impact of solution chemistry. *Journal of Colloid and Interface Science*, 485, 192–200. <https://doi.org/10.1016/j.jcis.2016.09.028>
- Liu, J., Wei, X., Xue, J., & Su, H. (2020). Preparation and adsorption properties of mesoporous material PS-MCM-41 with low-silicon content peanut shell ash as silicon source. *Materials Chemistry and Physics*, 241, 122355. <https://doi.org/10.1016/j.matchemphys.2019.122355>
- Liu, J., Chen, F., Li, C., Lu, L., Hu, C., Wei, Y., ... & Huang, Q. (2019). Characterization and utilization of industrial microbial waste as novel adsorbent to remove single and mixed dyes from water. *Journal of Cleaner Production*, 208, 552–562. <https://doi.org/10.1016/j.jclepro.2018.10.136>
- Liu, Y., Pan, Y., Wang, Z.-J., Kuai, P., & Liu, C.-J. (2010). Facile and fast template removal from mesoporous MCM-41 molecular sieve using dielectric-barrier discharge plasma. *Catalysis Communications*, 11(6), 551–554. <https://doi.org/10.1016/j.catcom.2009.12.017>
- Lopez, L., Montes, V., Kušar, H., Cabrera, S., Boutonnet, M., & Järås, S. (2016). Syngas conversion to ethanol over a mesoporous Cu/MCM-41 catalyst: Effect of K and Fe promoters. *Applied Catalysis A: General*, 526, 77–83. <https://doi.org/10.1016/j.apcata.2016.08.006>
- Luttrell, W. E. (2009). Acetaldehyde. *Journal of Chemical Health & Safety*, 16(5), 43–44.
- Medeiros, P. R., & Appel, L. G. (2002). The influence of the Ce–Mo–Sn preparation methods on ethanol oxidation. *Applied Catalysis A: General*, 231(1–2), 125–130. [https://doi.org/10.1016/S0926-860X\(02\)00075-3](https://doi.org/10.1016/S0926-860X(02)00075-3)
- Mohamed, R. M., Shawky, A., & Mkhallid, I. A. (2017). Facile synthesis of MgO and Ni-MgO nanostructures with enhanced adsorption of methyl blue dye. *Journal of Physics and Chemistry of Solids*, 101, 50–57. <https://doi.org/10.1016/j.jpics.2016.10.009>
- Mukherjee, S., Akshay, M., & Samanta, A. N. (2019). Amine-impregnated MCM-41 in post-combustion CO<sub>2</sub> capture: Synthesis, characterization, isotherm modelling. *Advanced Powder Technology*, 30(12), 3231–3240. <https://doi.org/10.1016/j.apt.2019.09.032>
- Peng, W., Li, J., Chen, B., Wang, N., Luo, G., & Wei, F. (2016). Mesoporous MgO synthesized by a homogeneous-hydrothermal method and its catalytic performance on gas-phase acetone condensation at low temperatures. *Catalysis Communications*, 74, 39–42. <https://doi.org/10.1016/j.catcom.2015.11.001>
- Pires, E., Miranda, E., & Valença, G. (2002). Gas-phase enzymatic esterification on immobilized lipases in MCM-41 molecular sieves. *Applied Biochemistry and Biotechnology*, 98, 963–976. [https://doi.org/10.1007/978-1-4612-0119-9\\_78](https://doi.org/10.1007/978-1-4612-0119-9_78)
- Pirouzmand, M., Anakhaton, M. M., & Ghasemi, Z. (2018). One-step biodiesel production from waste cooking oils over metal incorporated MCM-41; positive effect of template. *Fuel*, 216, 296–300. <https://doi.org/10.1016/j.fuel.2017.11.138>
- Pirouzmand, M., Asadi, M., & Mohammadi, A. (2018). The remarkable activity of template-containing Mg/MCM-41 and Ni/MCM-41 in CO<sub>2</sub> sequestration. *Greenhouse Gases: Science and Technology*, 8(3), 462–468. <https://doi.org/10.1002/ghg.1753>
- Paloschi, R. S. (2002). *Acomplamento não Oxidativo de Metano sobre Metais Suportados em Sólidos Microporosos*. Universidade Estadual de Campinas.
- Ramazani, Z., Elhamifar, D., Norouzi, M., & Mirbagheri, R. (2019). Magnetic mesoporous MCM-41 supported boric acid: A novel, efficient and ecofriendly nanocomposite. *Composites Part B: Engineering*, 164, 10–17. <https://doi.org/10.1016/j.compositesb.2018.11.063>

- Rana, R. K., & Viswanathan, B. (1998). Mo incorporation in MCM-41 type zeolite. *Catalysis Letters*, 52, 25–29.  
<https://doi.org/10.1023/A:1019019403375>
- Rodriguez-Gomez, A., Holgado, J. P., & Caballero, A. (2017). Cobalt Carbide Identified as Catalytic Site for the Dehydrogenation of Ethanol to Acetaldehyde. *ACS Catalysis*, 7(8), 5243–5247.  
<https://doi.org/10.1021/acscatal.7b01348>
- Rosales-Calderon, O., & Arantes, V. (2019). A review on commercial-scale high-value products that can be produced alongside cellulosic ethanol. *Biotechnology for Biofuels*, 12(1), 240.  
<https://doi.org/10.1186/s13068-019-1529-1>
- Safa, M. A., & Ma, X. (2016). Oxidation kinetics of dibenzothiophenes using cumene hydroperoxide as an oxidant over MoO<sub>3</sub>/Al<sub>2</sub>O<sub>3</sub> catalyst. *Fuel*, 171, 238–246.  
<https://doi.org/10.1016/j.fuel.2015.12.050>
- Santos, J. (2002). Catalytic Decomposition of Hydrazine on Tungsten Carbide: The Influence of Adsorbed Oxygen. *Journal of Catalysis*, 210(1), 1–6.  
<https://doi.org/10.1006/jcat.2002.3634>
- Saraiva, M. S., Fernandes, C. I., Nunes, T. G., Nunes, C. D., & Calhorda, M. J. (2014). New Mo(II) complexes in MCM-41 and silica: Synthesis and catalysis. *Journal of Organometallic Chemistry*, 751, 443–452.  
<https://doi.org/10.1016/j.jorganchem.2013.07.081>
- Shan, J., Janvelyan, N., Li, H., Liu, J., Egle, T. M., Ye, J., ... & Flytzani-Stephanopoulos, M. (2017). Selective non-oxidative dehydrogenation of ethanol to acetaldehyde and hydrogen on highly dilute NiCu alloys. *Applied Catalysis B: Environmental*, 205, 541–550.  
<https://doi.org/10.1016/j.apcatb.2016.12.045>
- Shan, J., Liu, J., Li, M., Lustig, S., Lee, S., & Flytzani-Stephanopoulos, M. (2018). NiCu single atom alloys catalyze the CH bond activation in the selective non-oxidative ethanol dehydrogenation reaction. *Applied Catalysis B: Environmental*, 226, 534–543.  
<https://doi.org/10.1016/j.apcatb.2017.12.059>
- Sharma, L., & Kakkar, R. (2017). Hierarchically structured magnesium based oxides: synthesis strategies and applications in organic pollutant remediation. *CrystEngComm*, 19(46), 6913–6926.  
<https://doi.org/10.1039/C7CE01755C>
- Sikarwar, P., Kumar, U. K. A., Gosu, V., & Subbaramaiah, V. (2018). Catalytic oxidative desulfurization of DBT using green catalyst (Mo/MCM-41) derived from coal fly ash. *Journal of Environmental Chemical Engineering*, 6(2), 1736–1744.  
<https://doi.org/10.1016/j.jece.2018.02.021>
- Stefanidis, S. D., et al. (2016). Natural magnesium oxide (MgO) catalysts: A cost-effective sustainable alternative to acid zeolites for the in situ upgrading of biomass fast pyrolysis oil. *Applied Catalysis B: Environmental*, 196, 155–173.  
<https://doi.org/10.1016/j.apcatb.2016.05.031>
- Sun, J., & Wang, Y. (2014). Recent Advances in Catalytic Conversion of Ethanol to Chemicals. *ACS Catalysis*, 4(4), 1078–1090.  
<https://doi.org/10.1021/cs4011343>
- Uphade, B. ., Yamada, Y., Akita, T., Nakamura, T., & Haruta, M. (2001). Synthesis and characterization of Ti-MCM-41 and vapor-phase epoxidation of propylene using H<sub>2</sub> and O<sub>2</sub> over Au/Ti-MCM-41. *Applied Catalysis A: General*, 215(1–2), 137–148.  
[https://doi.org/10.1016/S0926-860X\(01\)00527-0](https://doi.org/10.1016/S0926-860X(01)00527-0)
- Vinu, A., Ariga, K., Saravanamurugan, S., Hartmann, M., & Murugesan, V. (2004). Synthesis of highly acidic and well ordered MgAl-MCM-41 and its catalytic performance on the isopropylation of m-cresol. *Microporous and mesoporous materials*, 76(1-3), 91–98.  
<https://doi.org/10.1016/j.micromeso.2004.07.036>
- Wang, T., Wu, G., Guan, N., & Li, L. (2012). Nitridation of MgO-loaded MCM-41 and its beneficial applications in base-catalyzed reactions. *Microporous and Mesoporous Materials*, 148(1), 184–190.  
<https://doi.org/10.1016/j.micromeso.2011.07.024>
- Yang, R., Li, D., Li, A., & Yang, H. (2018). Adsorption properties and mechanisms of palygorskite for removal of various ionic dyes from water. *Applied Clay Science*, 151, 20–28.  
<https://doi.org/10.1016/j.clay.2017.10.016>

Yasyerli, S., Filizgok, S., Arbag, H., Yasyerli, N., & Dogu, G. (2011). Ru incorporated Ni-MCM-41 mesoporous catalysts for dry reforming of methane: Effects of Mg addition, feed composition and temperature. *International Journal of Hydrogen Energy*, 36(8), 4863-4874.

<https://doi.org/10.1016/j.ijhydene.2011.01.120>

Zhang, J., Kanno, M., Zhang, J., Ohnishi, R., Toriyabe, K., Matsuhashi, H., & Kamiya, Y. (2010). Preferential oligomerization of isobutene in a mixture of isobutene and 1-butene over sodium-modified 12-tungstosilicic acid supported on silica. *Journal of Molecular Catalysis A: Chemical*, 326(1-2), 107-112.

<https://doi.org/10.1016/j.molcata.2010.04.017>

Zhao, L., Sotoodeh, F., & Smith, K. J. (2010). Increased surface area of unsupported Mo<sub>2</sub>C catalyst by alkali-treatment. *Catalysis Communications*, 11(5), 391-395.

<https://doi.org/10.1016/j.catcom.2009.11.008>

Zheng, J., Chen, Z., Fang, J., Wang, Z., & Zuo, S. (2020). MCM-41 supported nano-sized CuO-CeO<sub>2</sub> for catalytic combustion of chlorobenzene. *Journal of Rare Earths*, 38(9), 933-940.

<https://doi.org/10.1016/j.jre.2019.06.005>